An Efficient Numerical Algorithm for Cracks Partly in Frictionless Contact

Helsing, Johan; Peters, Gunnar

Published in:
SIAM Journal on Applied Mathematics

DOI:
10.1137/S0036139999356934

2000

SIAM J. APPL. MATH.
Vol. 61, No. 2, pp. 551–566

AN EFFICIENT NUMERICAL ALGORITHM FOR CRACKS PARTLY IN FRICTIONLESS CONTACT*

JOHAN HELSING† AND GUNNAR PETERS‡

Abstract. An algorithm for a loaded crack partly in frictionless contact is presented. The problem is nonlinear in the sense that the equations of linear elasticity are supplemented by certain contact inequalities. The location of a priori unknown contact zones and the solutions to the field equations must be determined simultaneously. The algorithm is based on a rapidly converging sequence of relaxed Fredholm integral equations of the second kind in which the contact problem is viewed as a perturbation of a noncontacting crack problem. The algorithm exhibits great stability and speed. The numerical results are orders-of-magnitudes more accurate than those of previous investigators.

Key words. cracks, contact, contact zone, integral equations of Fredholm type, numerical methods, linear elasticity

AMS subject classifications. 73C02, 31A10, 45E05, 65R20

PII. S0036139999356934

1. Introduction.

Contact problems often arise in fracture mechanics. They are regarded as difficult. Suppose that we want to determine the stress field around a crack in planar linear elasticity. In the special cases of a straight crack or a circular arc–shaped crack and a load that keeps the crack completely open, there are simple analytical solutions [9, 11]. In a more general situation the load might be such that parts of the crack are in contact after its application. The problem is now nonlinear and an iterative numerical procedure is needed. A common simplification is to ignore the contact zones in order to save the linear nature of the problem. Such a practice causes errors. It could even suggest a different nature of the mode of fracture and lead to great uncertainty about the validity of theoretical models as experiments are compared to numerical predictions [12].

While finite element methods, involving contact nodes and possibly also penalty methods, are applicable for contact problems [8], many popular algorithms are based on complex potentials and integral equations. Chao and Laws [1], in a typical example, treat a circular arc–shaped crack under remote uniaxial loading. The setup is such that a part of the crack is in frictionless contact. The stress field is computed by iteratively solving a system of singular integral equations supplemented by a contact condition. The authors report several difficulties related to instabilities of their algorithm, including problems with determination of the actual contact length and significant computing costs.

Most commonly, contact problems in fracture mechanics are not ill-conditioned. The difficulty lies in finding a stable iterative numerical algorithm. Instabilities occur for two reasons: First, a mathematical description of the contact problem naturally leads to a system of singular integral equations of Fredholm's first kind. Such equa-

*Received by the editors June 2, 1999; accepted for publication (in revised form) November 2, 1999; published electronically August 3, 2000. This research was supported by NFR, TFR, and The Knut and Alice Wallenberg Foundation under TFR contract 96-977.

http://www.siam.org/journals/siap/61-2/35693.html

†Department of Solid Mechanics and NADA, Royal Institute of Technology, SE-100 44 Stockholm, Sweden (helsing@nada.kth.se).

‡Department of Mathematics, Royal Institute of Technology, SE-100 44 Stockholm, Sweden (peters@math.kth.se).

tions lead to unstable algorithms. Second, the locations of contact zones are the natural variables for iteration. In order to get a smooth solution one needs to introduce certain weights. Unfortunately, the solution of the naturally occurring integral equations has an asymptotic shape that is dependent on whether assumed contact zones have correct locations. Therefore, a weight that is suitable at an early stage of the iteration may be completely wrong at a later stage of the iteration.

2. Results. This paper presents a stable and efficient numerical algorithm for the calculation of the stress fields and precise locations of the contact zones for loaded cracks of general shapes. In an example, where a finite element method gives a 2% error for the contact zone, our algorithm produces 13 accurate digits in approximately one second on a regular workstation. See Example 4 in section 11.

Our approach consists of two major steps. The first step is to rewrite the basic equations as a system of Fredholm integral equations of the second kind. Well-conditioned Fredholm equations of the second kind can be solved with extreme accuracy in finite-dimensional subspaces of low dimension [6] and are, therefore, a preferred choice for numerical computations [13]. In the case of cracks in frictionless contact, the main obstacle is that the interaction between the contact zones and the noncontact zones is too strong to be described by compact integral operators. We solve this problem by rewriting the contacting crack problem as a perturbation of a noncontacting crack problem on the entire crack and an easier problem on the contact zones. This perturbation is small in the sense that the coupling between the two problems is given by compact integral operators. It is, however, equivalent to the original problem. The noncontacting problem was solved in [3].

The second step is to enhance numerical quadrature and other basic operations by introducing weights that compensate the singular behavior of the solution. In our case, the stress field has inverse square root singularities at the crack tips and square root behavior near the endpoints of the contact zones [11]. Both these behaviors are bad for numerics. Here the main problem is that in the iterative process of finding the exact positions of the contact zones, we encounter intermediate results with very different asymptotic behavior. This problem has been solved by relaxing the integral equations while introducing new constraints. In this new formulation all intermediate results have the same asymptotics as the true solution.

We give

- a reformulation of the integral equations appearing into a system of Fredholm equations of the second kind, that is, both stable and easy to use in an efficient way;
- the correct way to handle the asymptotics on the contact zones;
- an efficient algorithm for the problem at hand;
- particularities of the implementation of the algorithm;
- numerical examples with unprecedented numerical accuracy.

The paper is organized as follows. In section 3 we derive the basic integral equations for our problem. In sections 4 and 5 we reformulate these equations into a perturbation of a noncontacting crack problem, and in section 7 we derive a formulation as a system of Fredholm integral equations of the second kind. Section 6 contains some useful identities for the integral operators used. The final algorithm is presented in section 8. Sections 9 and 10 contain particularities of the implementation of this algorithm, and section 11 gives some numerical examples.

3. Basic equations. A material consists of an infinite medium with elastic moduli κ and μ which surrounds one crack. We denote the crack by Γ. The starting point and the endpoint of the crack, the so-called crack tips, are denoted γ_s and γ_e. Of special interest are two a priori unknown interior points on Γ denoted γ_1 and γ_2. The crack is open between γ_s and γ_1, in frictionless contact between γ_1 and γ_2, and open again between γ_2 and γ_e. The part of the crack that is in contact is denoted Γ_{co}. The normal traction on Γ_{co} is negative. The stress state at infinity is $\sigma^\infty = (\sigma_{xx}, \sigma_{yy}, \sigma_{xy})$. We will compute the stress and strain fields in this material subject to three different imposed stresses at infinity, namely $\sigma_{\mathrm{I}}^\infty = (1,0,0)$, $\sigma_{\mathrm{II}}^\infty = (0,1,0)$, and $\sigma_{\mathrm{III}}^\infty = (0,0,1)$.

It can be shown [11] that the stress field σ is given by a biharmonic function U called the Airy stress function:

$$\sigma_{xx} = \frac{\partial^2 U}{\partial y^2}, \ \sigma_{yy} = \frac{\partial^2 U}{\partial x^2}, \ \sigma_{xy} = -\frac{\partial^2 U}{\partial x \partial y}\,. \tag{1}$$

A standard starting point for crack problems in planar elasticity is to represent the Airy stress function as

$$U = \Re\mathrm{e}\left\{\bar{z}\phi + \chi\right\}, \tag{2}$$

where ϕ and χ are single valued analytic functions outside the crack. Following Muskhelishvili [11] we introduce the potentials $\psi = \chi'$, $\Phi = \phi'$, and $\Psi = \psi'$. It is natural to represent the uppercase potentials Φ and Ψ as Cauchy-type integrals

$$\Phi(z) = \frac{1}{2\pi i}\int_\Gamma \frac{\rho(\tau)\Omega(\tau)\mathrm{d}\tau}{(\tau - z)} + \frac{\alpha}{2} \tag{3}$$

and

$$\Psi(z) = \frac{1}{2\pi i}\int_\Gamma \frac{\rho(\tau)\Xi(\tau)\mathrm{d}\tau}{(\tau - z)} + \beta\,, \tag{4}$$

where $\Omega(z)$ and $\Xi(z)$ are unknown densities on Γ. In (3) and (4) $\rho(z)$ is a weight function on Γ, capturing the asymptotic behavior of the solution, and given by

$$\rho(z) = ((z-\gamma_s)(z-\gamma_e))^{-\frac{1}{2}}, \qquad z \in \Gamma. \tag{5}$$

To be precise, the weight function $\rho(z)$ is the limit from the right (relative to the orientation of the crack) of the branch given by a branch cut along Γ and

$$\lim_{z\to\infty} z\rho(z) = 1\,. \tag{6}$$

The densities Ω and Ξ of (3) and (4) need not be treated as independent variables. The requirement of continuity of the traction across the crack allows us to express Ξ as a function of Ω:

$$\rho(z)\Xi(z) = \frac{\bar{n}}{n}\overline{\rho(z)\Omega(z)} + \frac{\bar{n}}{n}\rho(z)\Omega(z) - \bar{z}(\rho(z)\Omega(z))'\,. \tag{7}$$

Therefore Ψ assumes the form

$$\Psi(z) = -\frac{1}{2\pi i}\int_\Gamma \frac{\overline{\rho(\tau)\Omega(\tau)}\mathrm{d}\bar{\tau}}{(\tau - z)} - \frac{1}{2\pi i}\int_\Gamma \frac{\bar{\tau}\rho(\tau)\Omega(\tau)\mathrm{d}\tau}{(\tau - z)^2} + \beta\,. \tag{8}$$

As discussed in [3], for a noncontacting crack problem the ansatz in (3) and (8) makes the solution Ω a smooth function. The weight ρ also appears in the definition of the integral operators below and its use in crack problems goes back to Muskhelishvili [11].

The choice (8) for Ψ was first suggested by Theocaris and Ioakimidis [16] and subsequently used by Greengard and Helsing [2] and Helsing and Peters [3]. A similar choice for the potential ψ was suggested by Sherman [15].

The constants α and β in (3) and (8) represent the forcing terms in our formulation. For imposed average stresses $\sigma_{\mathrm{I}}^{\infty}$, $\sigma_{\mathrm{II}}^{\infty}$, and $\sigma_{\mathrm{III}}^{\infty}$, the constants take the values $\alpha = 1/2$ and $\beta = -1/2$, $\alpha = 1/2$ and $\beta = 1/2$, and $\alpha = 0$ and $\beta = i$. Thus, α can always be assumed to be real, while β is either a real or an imaginary number.

Once Φ is assumed to take the form (3), the expression (8) for Ψ enforces continuity of the traction across the crack. The remaining physical requirements on the loaded crack take the form of the integral equations (14)–(18) below.

First we define the integral operators

$$M_1\Omega(z) = \frac{1}{\pi i}\int_\Gamma \frac{\rho(\tau)\Omega(\tau)\mathrm{d}\tau}{(\tau - z)}\,, \tag{9}$$

$$\begin{aligned} M_3\Omega(z) = \frac{1}{2\pi i}\Bigg[&\int_\Gamma \frac{\rho(\tau)\Omega(\tau)\mathrm{d}\tau}{(\tau - z)} + \frac{\bar{n}}{n}\int_\Gamma \frac{\rho(\tau)\Omega(\tau)\mathrm{d}\tau}{(\bar{\tau} - \bar{z})} \\ &+ \int_\Gamma \frac{\overline{\rho(\tau)\Omega(\tau)}\mathrm{d}\bar{\tau}}{(\bar{\tau} - \bar{z})} + \frac{\bar{n}}{n}\int_\Gamma \frac{(\tau - z)\overline{\rho(\tau)\Omega(\tau)}\mathrm{d}\bar{\tau}}{(\bar{\tau} - \bar{z})^2}\Bigg]\,, \end{aligned} \tag{10}$$

$$Qf = \frac{1}{\pi i}\int_\Gamma \rho(\tau) f(\tau)\mathrm{d}\tau\,, \tag{11}$$

and note that the crack-opening displacement and the traction along the crack are given by

$$\delta u + i\delta v = -\left(\frac{1}{\kappa} + \frac{1}{\mu}\right)\int_{\gamma_{\mathrm{s}}}^{z} \rho(\tau)\Omega(\tau)\mathrm{d}\tau\,, \tag{12}$$

$$t_x + it_y = n(M_1\Omega - M_3\Omega) - \bar{n}\bar{\beta} + n\alpha\,. \tag{13}$$

The physical requirements on the crack are given by the following five integral equations:

Zero traction on the open parts of the crack:

$$(M_1 - M_3)\,\Omega(z) = \frac{\bar{n}}{n}\bar{\beta} - \alpha\,, \qquad z \in \Gamma - \Gamma_{\mathrm{co}}\,. \tag{14}$$

Zero friction along the contact zone:

$$\Im\mathrm{m}\,\{(M_1 - M_3)\Omega(z)\} = \Im\mathrm{m}\left\{\frac{\bar{n}}{n}\bar{\beta} - \alpha\right\}, \qquad z \in \Gamma_{\mathrm{co}}\,. \tag{15}$$

Negative normal traction along the contact zone:

$$\Re\mathrm{e}\,\{(M_1 - M_3)\Omega(z)\} \leq \Re\mathrm{e}\left\{\frac{\bar{n}}{n}\bar{\beta} - \alpha\right\}, \qquad z \in \Gamma_{\mathrm{co}}\,. \tag{16}$$

Contact, that is, zero normal crack-opening displacement along the contact zone:

$$\Re\mathrm{e}\left\{\bar{n}\int_{\gamma_{\mathrm{s}}}^{z} \rho(\tau)\Omega(\tau)\mathrm{d}\tau\right\} = 0\,, \qquad z \in \Gamma_{\mathrm{co}}\,. \tag{17}$$

Closure of the crack:

$$Q\Omega = 0\,. \tag{18}$$

For future reference we also introduce the integral operator M_4 given by

$$M_4 f(z) = \frac{1}{\pi i}\int_\Gamma \frac{f(\tau)\mathrm{d}\tau}{\rho(\tau)(\tau - z)}\,, \qquad z \in \Gamma\,. \tag{19}$$

The relation of M_4 to M_1 is thoroughly discussed in [3]. See also section 6.

4. A model problem. To illustrate the idea behind the particular choice of integral equation in the next section, we solve a simple model problem:

$$\begin{aligned} \Re\mathrm{e}\,\{M_1 T\} &= f\,,\\ \Re\mathrm{e}\,\{\rho T\} &= 0\,,\\ QT &= 0\,. \end{aligned} \tag{20}$$

Using the analysis in [3] this can be written as

$$\begin{aligned} T - iM_4\Im\mathrm{m}\,\{M_1 T\} &= M_4 f\,,\\ \Re\mathrm{e}\,\{\rho T\} &= 0\,. \end{aligned} \tag{21}$$

We have the following theorem.

Theorem 1. *The system of equations* (20) *is equivalent to*

$$T - iM_4\Im\mathrm{m}\left\{M_1\rho^{-1}i\Im\mathrm{m}\,\{\rho T\}\right\} = M_4 f\,. \tag{22}$$

Proof. Equation (22) obviously follows from (21) and therefore from (20). Now let T be the solution of (22). We then have (see Lemma 3)

$$M_1 T - i\Im\mathrm{m}\left\{M_1\rho^{-1}i\Im\mathrm{m}\,\{\rho T\}\right\} = f \tag{23}$$

and trivially

$$M_1 T - i\Im\mathrm{m}\left\{M_1\rho^{-1}\rho T\right\} = \Re\mathrm{e}\,\{M_1 T\}\,. \tag{24}$$

Since the right-hand sides in both (23) and (24) are real, they must be equal. We conclude that

$$\Re\mathrm{e}\,\{M_1 T\} = f\,, \tag{25}$$

$$\Im\mathrm{m}\left\{M_1\rho^{-1}\Re\mathrm{e}\,\{\rho T\}\right\} = 0\,. \tag{26}$$

Equation (22) also implies

$$QT = 0\,. \tag{27}$$

We now map the exterior of the crack conformally onto the exterior of an interval of the real line. Using complex analytic function theory, it is possible to show that the problem of solving (26) maps onto a similar problem on this interval. This is nontrivial in the sense that the conformal mapping does not extend to a unique mapping on the crack, since we have a so-called welding problem. The new problem on the interval, together with results from [3], implies

$$\Re\mathrm{e}\{\rho T\} = 0\,. \tag{28}$$

This proves that (22) implies (20). $\square$

We point out that numerical algorithms based on integral equations of Fredholm's second kind tend to be very stable.

5. Perturbation of the noncontacting crack problem. Consider now the system (14)–(18). If we have no contact zone, that is, $\Gamma_{\mathrm{co}} = \emptyset$, this is a noncontacting crack problem. The basic idea is to treat the problem at hand as a perturbation of a noncontacting crack problem, which was solved in [3]. The solution of the noncontacting problem and the fact that the null-space of Q is the image of M_4 (see [3]) suggests the following splitting of the solution Ω:

$$\Omega_I = M_4 \left(M_3\Omega + \frac{\bar{n}}{n}\bar{\beta} - \alpha \right) , \tag{29}$$

$$\Omega = \Omega_{\mathrm{I}} + M_4 T_0 \, , \tag{30}$$

where Ω_I and T_0 are two new functions along Γ, for which we have to solve.

The system (14)–(18) now takes the form

$$T_0 = 0 \, , \qquad z \in \Gamma \ \setminus \Gamma_{\mathrm{co}} \, , \tag{31}$$

$$\Im\mathrm{m} \{T_0\} = 0 \, , \qquad z \in \Gamma_{\mathrm{co}} \, , \tag{32}$$

$$\Re\mathrm{e} \{T_0\} \leq 0 \, , \qquad z \in \Gamma_{\mathrm{co}} \, , \tag{33}$$

$$\Re\mathrm{e} \left\{ \bar{n} \int_{\gamma_{\mathrm{s}}}^{z} \rho(\Omega_{\mathrm{I}} + M_4 T_0) \mathrm{d}\tau \right\} = 0 \, , \qquad z \in \Gamma_{\mathrm{co}} \, . \tag{34}$$

Equation (34) can be written

$$\bar{n} \int_{\gamma_{\mathrm{s}}}^{z} \rho(\Omega_{\mathrm{I}} + M_4 T_0) \mathrm{d}\tau - i \Im\mathrm{m} \left\{ \bar{n} \int_{\gamma_{\mathrm{s}}}^{z} \rho(\Omega_{\mathrm{I}} + M_4 T_0) \mathrm{d}\tau \right\} = 0 \, , \qquad z \in \Gamma_{\mathrm{co}} \, , \tag{35}$$

and the following lemma shows that replacing T_0 by $\Re\mathrm{e}\ \{T_0\}$ in the second term of (35) makes (32) redundant.

Lemma 2. *If T_0 solves the integral equation*

$$\begin{aligned} \bar{n} \int_{\gamma_{\mathrm{s}}}^{z} & \rho \ (\Omega_{\mathrm{I}} + M_4 T_0) \mathrm{d}\tau \\ & - i \Im\mathrm{m} \left\{ \bar{n} \int_{\gamma_{\mathrm{s}}}^{z} \rho(\Omega_{\mathrm{I}} + M_4 \Re\mathrm{e}\ \{T_0\}) \mathrm{d}\tau \right\} = 0 \, , \qquad z \in \Gamma_{\mathrm{co}} \, , \end{aligned} \tag{36}$$

then

$$\Im\mathrm{m}\ \{T_0\} \equiv 0 \, .$$

We define the weight

$$\eta(z) = ((z-\gamma_1)(z-\gamma_2))^{-\frac{1}{2}} \, , \qquad z \in \Gamma \, , \tag{37}$$

and, motivated by the final form of the solution given in section 7, we introduce η and ρ into the equations and write $T_0 = \rho T/\eta$. This makes the solution T a smooth function on Γ_{co}. See section 6 for more details on the weight η. We end up with the following system of equations:

$$\Omega_{\mathrm{I}} - M_4 M_3 (\Omega_{\mathrm{I}} + M_4 \Re\mathrm{e}\ \{\rho T/\eta\}) = M_4 \left(\frac{\bar{n}}{n}\bar{\beta} - \alpha \right) , \qquad z \in \Gamma \, , \tag{38}$$

$$\Re\mathrm{e}\ \{\rho T/\eta\} \leq 0 \, , \qquad z \in \Gamma_{\mathrm{co}} \, , \tag{39}$$

$$\begin{aligned} \bar{n} \int_{\gamma_{\mathrm{s}}}^{z} & \rho(\Omega_{\mathrm{I}} + M_4 \rho T/\eta) \mathrm{d}\tau \\ - i \, \Im\mathrm{m} & \left\{ \bar{n} \int_{\gamma_{\mathrm{s}}}^{z} \rho(\Omega_{\mathrm{I}} + M_4 \Re\mathrm{e}\ \{\rho T/\eta\}) \mathrm{d}\tau \right\} = 0 \, , \qquad z \in \Gamma_{\mathrm{co}} \, , \end{aligned} \tag{40}$$

where Ω_I is a function on Γ, while T is a function on Γ_{co}.

6. Hilbert space formulation of the problem. As in [3] we denote $\nu = |\rho|$ and introduce the Hilbert space of functions along Γ:

$$L^2(\nu, \Gamma) = \left\{ f : \int_\Gamma |f|^2 \nu ds < \infty \right\} . \tag{41}$$

We also write

$$L^2(\nu, \Gamma_{\text{co}}) = \left\{ f \in L^2(\nu, \Gamma) : f(z) = 0, \quad z \in \Gamma \setminus \Gamma_{\text{co}} \right\} . \tag{42}$$

We will solve the system (38)–(40) for $(\Omega_I, T) \in L^2(\nu, \Gamma) \times L^2(\nu, \Gamma_{\text{co}})$. A short motivation for using this kind of weighted space is that, since ρ is a Muckenhoupt weight [10], the Cauchy-type integrals remain bounded while operators such as M_3 and Q become compact; see [3]. For these results to hold it is sufficient that Γ is a C^2 curve.

Let M_4 be as in (19) and denote

$$t_{\text{cr}} = \frac{\gamma_{\text{s}} + \gamma_{\text{e}}}{2} . \tag{43}$$

The following lemma was proved in [3].

Lemma 3.

$$QM_4 f(z) = 0 , \qquad f \in L^2(\nu, \Gamma) , \tag{44}$$

$$M_1 \circ M_4 f(z) = f(z) , \tag{45}$$

$$M_4 \circ M_1 f(z) = f(z) - Qf , \tag{46}$$

$$M_4 1 = z - t_{\text{cr}} . \tag{47}$$

Similar operators can be defined on $L^2(\nu, \Gamma_{\text{co}})$. Let η be the weight defined in (37) and define operators

$$M_5 f(z) = \frac{1}{\pi i} \int_{\Gamma_{\text{co}}} \frac{\eta(\tau) f(\tau) \mathrm{d}\tau}{(\tau - z)} , \qquad z \in \Gamma_{\text{co}} , \tag{48}$$

$$M_6 f(z) = \frac{1}{\pi i} \int_{\Gamma_{\text{co}}} \frac{f(\tau) \mathrm{d}\tau}{\eta(\tau)(\tau - z)} , \qquad z \in \Gamma_{\text{co}} , \tag{49}$$

and a constant t_{co}

$$t_{\text{co}} = \frac{\gamma_1 + \gamma_2}{2} . \tag{50}$$

We then have the following lemma.

Lemma 4.

$$M_5 1 = 0 , \qquad z \in \Gamma_{\text{co}} , \tag{51}$$

$$M_6 1 = z - t_{\text{co}} , \qquad z \in \Gamma_{\text{co}} , \tag{52}$$

$$M_5 \circ M_6 f(z) = f(z) , \qquad z \in \Gamma_{\text{co}} . \tag{53}$$

We will sometimes write $M_5 f$, even if $f \in L^2(\nu, \Gamma)$. By this we will mean M_5 acting on the restriction of f to Γ_{co}. The result will be viewed as a function in $L^2(\nu, \Gamma_{\text{co}})$. Also we will need the new weight $\eta(z)$ for $z \in \Gamma \setminus \Gamma_{\text{co}}$. See section 9 for further details on the weights and section 10 for particularities of the numerical evaluation of singular integrals.

7. Fredholm equations of the second kind. Since we will solve the system (38)–(40) for $(\Omega_I, T) \in L^2(\nu, \Gamma) \times L^2(\nu, \Gamma_{\rm co})$, we want to rewrite it as a system of Fredholm integral equations of the second kind on this Hilbert space. First we note that M_3 is compact while M_4 is bounded on this Hilbert space. Therefore (38) is already of the second kind, and we concentrate on (40).

Let s be the arclength parameter along the crack and write $dz = in(z)ds$. Differentiating (40) with respect to s implies

$$\begin{aligned}(54)\qquad &\Omega_{\rm I} + M_4\rho T/\eta \\ &-\frac{1}{\rho}\frac{\rm d}{n{\rm d}s}\left[n\Im{\rm m}\left\{\bar{n}\int_{\gamma_{\rm s}}^{z}\rho(\Omega_{\rm I} + M_4\Re{\rm e}\ \{\rho T/\eta\}){\rm d}\tau\right\}\right] = 0\,, \qquad z \in \Gamma_{\rm co}\,,\end{aligned}$$

$$(55)\qquad \Re{\rm e}\left\{\bar{n}(\gamma_1)\int_{\gamma_{\rm s}}^{\gamma_1}\rho(\Omega_{\rm I} + M_4\Re{\rm e}\ \{\rho T/\eta\}){\rm d}\tau\right\} = 0\,.$$

Since $T(z) = 0$ for $z \notin \Gamma_{\rm co}$, (53) implies that we have $M_5 M_4 \rho T/\eta = T$. We obtain

$$\begin{aligned}(56)\quad &T - M_5\frac{1}{\rho}\frac{\rm d}{n{\rm d}s}\left[n\Im{\rm m}\left\{\bar{n}\int_{\gamma_{\rm s}}^{z}\rho(\Omega_{\rm I} + M_4\Re{\rm e}\ \{\rho T/\eta\}){\rm d}\tau\right\}\right] \\ &+M_5M_4M_3(\Omega_I + M_4\Re{\rm e}\ \{\rho T/\eta\}) = -M_5M_4\left(\frac{\bar{n}}{n}\bar{\beta} - \alpha\right), \qquad z \in \Gamma_{\rm co}\,,\end{aligned}$$

$$(57)\qquad \Re{\rm e}\left\{\bar{n}(\gamma_1)\int_{\gamma_{\rm s}}^{\gamma_1}\rho(\Omega_{\rm I} + M_4\Re{\rm e}\ \{\rho T/\eta\}){\rm d}\tau\right\} = 0\,.$$

However, this formulation is not equivalent to (54), (55). The operator M_5 has a kernel consisting exactly of functions that are constant along $\Gamma_{\rm co}$. This implies that (56) is equivalent to the following weaker form of (54):

$$\begin{aligned}(58)\qquad &\Omega_{\rm I} + M_4\rho T/\eta \\ &-\frac{1}{\rho}\frac{\rm d}{n{\rm d}s}\left[\Im{\rm m}\left\{\bar{n}\int_{\gamma_{\rm s}}^{z}\rho(\Omega_{\rm I} + M_4\Re{\rm e}\ \{\rho T/\eta\}){\rm d}\tau\right\}\right] = c\,, \qquad z \in \Gamma_{\rm co}\,,\end{aligned}$$

where c is a constant given by a consistency condition. If we add the equation

$$(59)\qquad \Re{\rm e}\left\{\bar{n}(\gamma_2)\int_{\gamma_{\rm s}}^{\gamma_2}\rho(\Omega_{\rm I} + M_4\Re{\rm e}\ \{\rho T/\eta\}){\rm d}\tau\right\} = 0\,,$$

which is also implied by (40), then the constant c must be zero. Finally, we replace Ω_I in (58) with the expression given in (29). This gives us the following theorem.

THEOREM 5. *The system* (38)–(40) *is equivalent to the following system of Fredholm integral equations of the second kind:*

$$(60)\qquad \Omega_I - M_4M_3\left(\Omega_I + M_4\Re{\rm e}\ \{\rho T/\eta\}\right) = M_4\left(\frac{\bar{n}}{n}\bar{\beta} - \alpha\right)\,, \qquad z \in \Gamma\,,$$

$$\begin{aligned}(61)\qquad &T + M_5M_4M_3(\Omega_I + M_4\Re{\rm e}\ \{\rho T/\eta\}) \\ &-M_5\frac{1}{\rho}\frac{\rm d}{n{\rm d}s}\left[n\Im{\rm m}\left\{\bar{n}\int_{\gamma_{\rm s}}^{z}\rho M_4\left(M_3\left(\Omega_I + M_4\Re{\rm e}\ \{\rho T/\eta\}\right) + \Re{\rm e}\ \{\rho T/\eta\}\right){\rm d}\tau\right\}\right] \\ &= M_5\frac{1}{\rho}\frac{\rm d}{n{\rm d}s}\left[n\Im{\rm m}\left\{\bar{n}\int_{\gamma_{\rm s}}^{z}\rho M_4\left(\frac{\bar{n}}{n}\bar{\beta} - \alpha\right){\rm d}\tau\right\}\right] - M_5M_4\left(\frac{\bar{n}}{n}\bar{\beta} - \alpha\right)\,, \qquad z \in \Gamma_{\rm co}\,,\end{aligned}$$

and the constraints

$$\Re\mathrm{e}\left\{\bar{n}(\gamma_1)\int_{\gamma_s}^{\gamma_1}\rho(\Omega_{\mathrm{I}}+M_4\Re\mathrm{e}\,\{\rho T/\eta\})\mathrm{d}\tau\right\}=0\,, \tag{62}$$

$$\Re\mathrm{e}\left\{\bar{n}(\gamma_2)\int_{\gamma_s}^{\gamma_2}\rho(\Omega_{\mathrm{I}}+M_4\Re\mathrm{e}\,\{\rho T/\eta\})\mathrm{d}\tau\right\}=0\,. \tag{63}$$

Proof. It remains to prove that in (60) and (61) the perturbations of the identity are compact operators. This follows by lengthy but straightforward calculations. The problem is mainly that M_5 is an unbounded operator. However, the explicit form of the kernels of the other operators allows us to show that the composition of M_5 with the various integral operators appearing in (60) and (61) are compact operators. □

Equations (60) and (61) constitute the basis for our numerical algorithm. It is worth pointing out that we do not implement these equations exactly as they stand. When M_3 is applied to $M_4\Re\mathrm{e}\,\{\rho T/\eta\}$ from the left, it will be difficult to compute $M_4\Re\mathrm{e}\,\{\rho T/\eta\}$ accurately for target points on $\Gamma\backslash\Gamma_{\mathrm{co}}$ close to γ_1 or γ_2, unless a smooth extension of T is known. To this end we extend the domain of validity for (61) and the support for T a few quadrature panels to the right and to the left of Γ_{co}. We also implement the differentiation operator in a particularly stable way. See section 10 for details.

We note that the original formulation (54), (55), apart from not being of the second kind, has the following drawback: If (62) and (63) are not fulfilled, then in (58) $c \neq 0$, and (54), (55) has no solution in $L^2(\nu,\Gamma)\times L^2(\nu,\Gamma_{\mathrm{co}})$. The iterative method designed below would therefore have to deal with very singular intermediate results.

8. The algorithm for the contacting problem. First note that the condition

$$\Re\mathrm{e}\,\{\rho T/\eta\}<0 \tag{64}$$

describes contact under negative normal traction. A nonnegative value of this expression indicates the splitting of Γ_{co} into several zones. We will describe the algorithm under the assumption of a single contact zone. A generalization to several contact zones is straightforward.

For given values of the endpoints γ_1 and γ_2 we solve the system (60), (61) using the GMRES iterative solver [14]. This can be accomplished with high accuracy and only a few iterations due to the fact that we use a formulation with Fredholm integral equations of the second kind. We then evaluate the two functions

$$f_1(\gamma_1,\gamma_2)=-\Re\mathrm{e}\left\{\bar{n}(\gamma_1)\int_{\gamma_s}^{\gamma_1}\rho(\Omega_{\mathrm{I}}+M_4\Re\mathrm{e}\,\{\rho T/\eta\})\mathrm{d}\tau\right\}\,, \tag{65}$$

$$f_2(\gamma_1,\gamma_2)=-\Re\mathrm{e}\left\{\bar{n}(\gamma_2)\int_{\gamma_s}^{\gamma_2}\rho(\Omega_{\mathrm{I}}+M_4\Re\mathrm{e}\,\{\rho T/\eta\})\mathrm{d}\tau\right\}\,. \tag{66}$$

The objective is to adjust γ_1 and γ_2 so that f_1 and f_2 of (65), (66) both become zero. This problem is solved using Broyden's method, which is a simple and effective secant updating method for solving nonlinear systems. The initial Jacobian approximation is taken as

$$J=\begin{bmatrix}-1 & 0\\ 0 & 1\end{bmatrix}. \tag{67}$$

If the initial guesses for γ_1 and γ_2 are reasonable, Broyden's method converges to the correct solution for (60)–(63) and, equivalently, for the original equations (14)–(18). In our implementation of the algorithm we determine the initial guesses for γ_1 and γ_2 by looking at the solution to the noncontacting crack problem (for which negative crack-opening displacement is allowed). The initial guesses are taken to be those points on the crack between which the normal component of the crack-opening displacement is negative.

9. Branch chasing for the contact zone. As in the case of a noncontacting crack [3], the weight $\eta(z)$ is defined by

$$\frac{1}{\eta(z)} = \chi(z) \cdot \mathrm{Sqrt}\,(z-\gamma_1)\mathrm{Sqrt}\,(z-\gamma_2)\,, \tag{68}$$

where Sqrt () is the principal branch of the square root given by a cut along the negative real axis and Sqrt (1) = 1. On the contact zone Γ_{co} the weight $\eta(z)$ is calculated in complete analogy with section 9.1 of [3]. Let η_1 and η_2 denote the limiting values of that calculation for the two endpoints γ_1 and γ_2, respectively, and define θ_1 and θ_2 as in [3].

We need to calculate $\eta(z)$ on the two segments of Γ that are not in contact. For the first segment set

$$\widetilde{\eta_1} = -i\eta_1\,.$$

The starting value for $\chi(z)$, as one goes backward from γ_1 towards γ_{s}, is given by

$$\widetilde{\chi_1} = \frac{1}{\widetilde{\eta_1}\mathrm{Sqrt}\,(z-\gamma_1)\mathrm{Sqrt}\,(z-\gamma_2)} \tag{69}$$

and $\chi(z)$ changes sign exactly when θ_1 or θ_2 passes through an odd multiple of π.

Going from γ_2 towards γ_{e}, the starting values are

$$\widetilde{\eta_2} = i\eta_2$$

and

$$\widetilde{\chi_2} = \frac{1}{\widetilde{\eta_2}\mathrm{Sqrt}\,(z-\gamma_1)\mathrm{Sqrt}\,(z-\gamma_2)}\,,$$

and the sign changes according to the same rules as above.

10. Numerical evaluation of singular integrals. Let f be a smooth function on Γ. We evaluate M_4 operating on f:

$$M_4\rho f/\eta(z) = \begin{cases} f(z)(z-t_{\mathrm{co}}) + \dfrac{1}{i\pi}\displaystyle\int_{\Gamma_{\mathrm{co}}} \frac{(f(\tau)-f(z))\mathrm{d}\tau}{\eta(\tau)(\tau-z)}\,, & z\in\Gamma_{\mathrm{co}}\,, \\[2ex] \tilde{f}(z)(z-t_{\mathrm{co}}) + \dfrac{\tilde{f}(z)}{\eta(z)} + \dfrac{1}{i\pi}\displaystyle\int_{\Gamma_{\mathrm{co}}} \frac{(f(\tau)-\tilde{f}(z))\mathrm{d}\tau}{\eta(\tau)(\tau-z)}, & z\in\tilde{\Gamma}_{\mathrm{co}}\setminus\Gamma_{\mathrm{co}}, \\[2ex] \dfrac{1}{i\pi}\displaystyle\int_{\Gamma_{\mathrm{co}}} \frac{f(\tau)\mathrm{d}\tau}{\eta(\tau)(\tau-z)}\,, & z\in\Gamma\setminus\tilde{\Gamma}_{\mathrm{co}}\,. \end{cases} \tag{70}$$

Here $\tilde{\Gamma}_{\mathrm{co}}$ is an extension of Γ_{co} with a few quadrature panels to the left and to the right, and $\tilde{f}$ is a smooth extension of f to $\tilde{\Gamma}_{\mathrm{co}}$.

Below we will denote by $\tilde{M}_5$ and $\tilde{M}_6$ the smooth extensions of M_5 and M_6 to $\tilde{\Gamma}_{\mathrm{co}}$, that is, the result of a smooth extension of the functions $M_5 f$ and $M_6 f$ to $\tilde{\Gamma}_{\mathrm{co}}$. Let f be a smooth function on Γ. We evaluate $\tilde{M}_5$ operating on f:

$$\tilde{M}_5 f(z) = \frac{1}{i\pi}\int_{\Gamma_{\mathrm{co}}} \frac{\eta(\tau)(f(\tau)-f(z))\mathrm{d}\tau}{(\tau - z)}\,, \qquad z \in \tilde{\Gamma}_{\mathrm{co}}\,. \tag{71}$$

Let f be a smooth function with support only on Γ_{co}. We evaluate $\tilde{M}_6$ operating on f

$$\tilde{M}_6 f(z) = \begin{cases} f(z)(z-t_{\mathrm{co}}) + \dfrac{1}{i\pi}\displaystyle\int_{\Gamma_{\mathrm{co}}} \frac{(f(\tau)-f(z))\mathrm{d}\tau}{\eta(\tau)(\tau-z)}\,, & z\in\Gamma_{\mathrm{co}}\,,\\ \tilde{f}(z)(z-t_{\mathrm{co}}) + \dfrac{1}{i\pi}\displaystyle\int_{\Gamma_{\mathrm{co}}} \frac{(f(\tau)-\tilde{f}(z))\mathrm{d}\tau}{\eta(\tau)(\tau-z)}\,, & z\in\tilde{\Gamma}_{\mathrm{co}}\setminus\Gamma_{\mathrm{co}}\,, \end{cases} \tag{72}$$

where $\tilde{f}(z)$ is a smooth extension of $f(z)$ to $\tilde{\Gamma}_{\mathrm{co}}$.

In terms of the extended operators introduced above, our implementation of (61) can be written

$$\begin{aligned} &\tilde{T} + \tilde{M}_5 M_4 M_3(\Omega_{\mathrm{II}} + M_4 \Re\mathrm{e}\{\rho T/\eta\}) \\ &-\tilde{M}_5 \frac{1}{\rho}\frac{\mathrm{d}}{n\mathrm{d}s}\left[n\Im\mathrm{m}\left\{\bar{n}\int_{\gamma_{\mathrm{s}}}^{\gamma_1} \rho M_4 \Re\mathrm{e}\{\rho T/\eta\}\mathrm{d}\tau\right\}\right] \\ &-\tilde{M}_5 \frac{1}{\rho}\frac{\mathrm{d}}{n\mathrm{d}s}\left[n\Im\mathrm{m}\left\{\bar{n}\int_{\gamma_1}^{z} \rho \tilde{M}_6 \eta/\rho \Re\mathrm{e}\{\rho T/\eta\}\mathrm{d}\tau\right\}\right] \\ &-\tilde{M}_5 \frac{1}{\rho}\frac{\mathrm{d}}{n\mathrm{d}s}\left[n\Im\mathrm{m}\left\{\bar{n}\int_{\gamma_{\mathrm{s}}}^{z} \rho M_4 M_3(\Omega_{\mathrm{II}} + M_4\Re\mathrm{e}\{\rho T/\eta\})\mathrm{d}\tau\right\}\right] \\ = &\tilde{M}_5 \frac{1}{\rho}\frac{\mathrm{d}}{n\mathrm{d}s}\left[n\Im\mathrm{m}\left\{\bar{n}\int_{\gamma_{\mathrm{s}}}^{z}\rho M_4\left(\frac{\bar{n}}{n}\bar{\beta}-\alpha\right)\mathrm{d}\tau\right\}\right] - \tilde{M}_5 M_4\left(\frac{\bar{n}}{n}\bar{\beta}-\alpha\right), \qquad z\in\tilde{\Gamma}_{\mathrm{co}}\,. \end{aligned} \tag{73}$$

The quantities upon which the differentiation operator in (73) act are smooth if γ_{s} differs from γ_1. If it should happen that γ_{s} and γ_1 are equal, they are not. Therefore, in the numerical implementation of (73), we also use the substitution

$$\frac{1}{\rho}\frac{\mathrm{d}f}{n\mathrm{d}s} = \frac{\mathrm{d}}{n\mathrm{d}s}\frac{f}{\rho} - i(z-t_{\mathrm{cr}})\rho f\,.$$

With this substitution the differentiation operator acts on a smooth quantity irrespective of the location of γ_{s} and γ_1.

11. Numerical examples. This section presents four examples where (60), (61) are solved numerically for easily reproduced setups. The algorithm is implemented using a Nyström scheme, based on 16-point composite Gaussian quadrature, the GMRES iterative solver [14], and the techniques discussed in section 10. The GMRES iterations are terminated when the residual is less than 10^{-14}, and that same tolerance is used as a stopping criterion for f_1 and f_2 of (65), (66) in the Broyden iterations. In Table 1 and Figure 5, where we seek highest possible accuracy, the tolerances are lowered to $5\cdot 10^{-16}$. Compensated summation [4, 7] is used whenever deemed necessary, for example, in the computation of matrix–vector multiplications and inner products in the GMRES iterative solver.

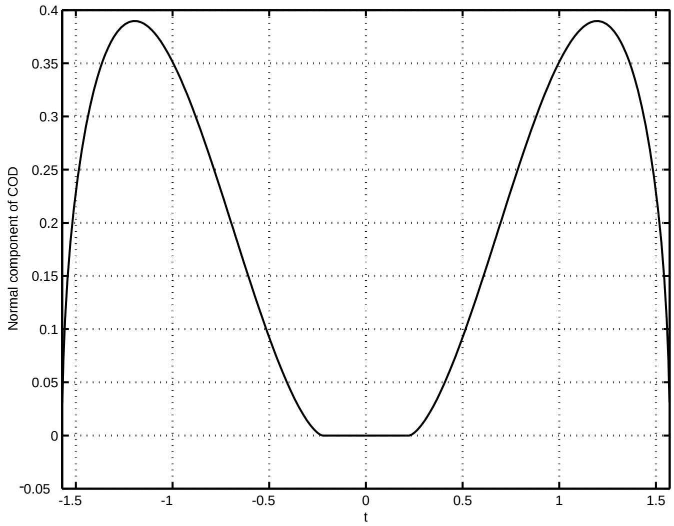

FIG. 1. *Example* 1*: The normal component of the crack-opening displacement versus arclength parameter $-\pi/2 \le t \le \pi/2$ for a unit semicircular crack subjected to a uniform stress $\sigma_{\mathrm{II}}^{\infty}$ at infinity.*

Example 1: Circular arc–shaped crack in symmetric contact. As a simple example we choose a crack parameterized by

$$z(t) = e^{it}\,, \qquad -\pi/2 \le t \le \pi/2\,. \tag{74}$$

The elastic moduli of the surrounding medium are $\kappa = 2$ and $\mu = 2$. A uniaxial stress $\sigma_{\mathrm{II}}^{\infty}$ is applied at infinity. This problem is very well conditioned. The GMRES iterative solver typically converges to a residual of 10^{-14} in nine iterations irrespective of the number of discretization points and the placement of the points γ_1 and γ_2. We choose $\gamma_1 = e^{-0.4i}$ and $\gamma_2 = e^{0.4i}$ as initial guesses. After six iterations with Broyden's method, and with 96 discretization points on Γ, we find that $\gamma_1 = e^{-it}$ and $\gamma_2 = e^{it}$, where $t = 0.2241658890840$, make the solution to (60), (61) satisfy (29) and (32)–(34) to at least 13 digits; see Figure 1. With 96 discretization points this calculation took four seconds on a SUN Ultra 10 workstation.

Example 2: Circular arc–shaped crack in asymmetric contact. In a second example we change the parameterization of the crack to

$$z(t) = e^{it}\,, \qquad -1 \le t \le 2\,. \tag{75}$$

This example is about as well conditioned as Example 1. We choose $\gamma_1 = e^{-0.9i}$ and $\gamma_2 = e^{0.3i}$ as initial guesses. The GMRES iterative solver typically converges to a residual of 10^{-14} in 11 iterations. After 12 iterations with Broyden's method, and with 176 discretization points on Γ, we find that $\gamma_1 = e^{it_1}$ and $\gamma_2 = e^{it_2}$, where $t_1 = -0.6649345251012$ and $t_2 = 0.1061303707331$ make the solution to (60), (61) satisfy (29) and (32)–(34); see Figure 2. With 176 discretization points this calculation took 15 seconds on a SUN Ultra 10 workstation.

Example 3: Contact in a crack with wavy shape. In a third example we change the parameterization of the crack to

$$z(t) = (1 + 0.2\cos 5t)e^{it}\,, \qquad 0.1 \le t \le 2.3\,. \tag{76}$$

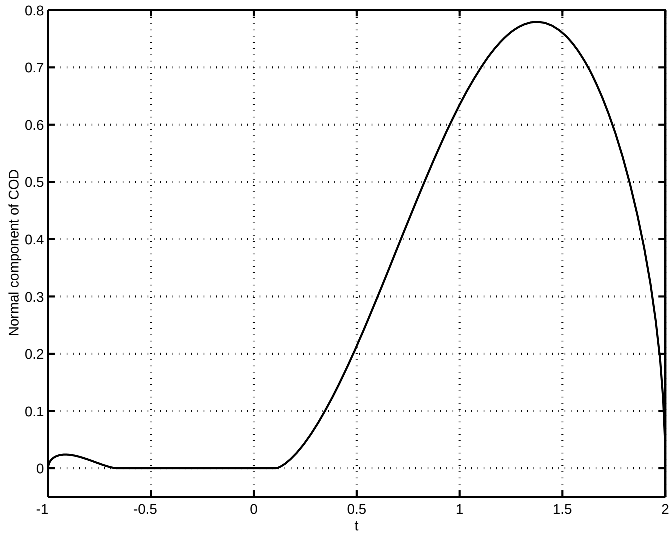

FIG. 2. *Example* 2*: The normal component of the crack-opening displacement versus arclength parameter* $-1 \leq t \leq 2$ *for a unit circular arc–shaped crack subjected to a uniform stress* $\sigma_{\mathrm{II}}^{\infty}$ *at infinity.*

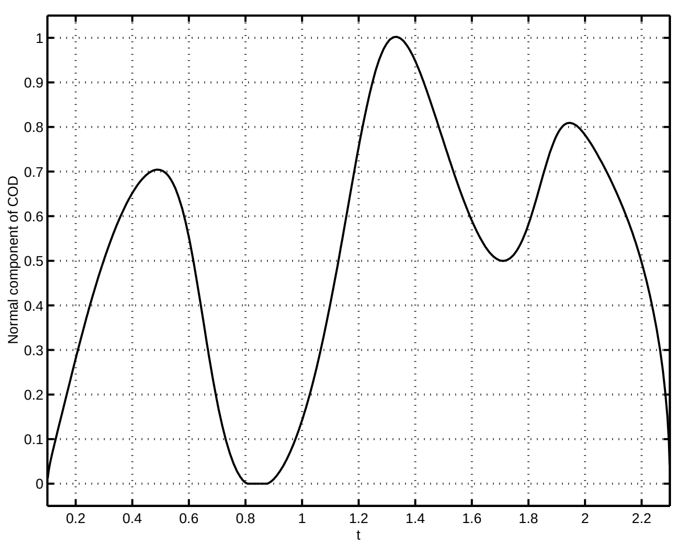

FIG. 3. *Example* 3*: The normal component of the crack-opening displacement versus arclength parameter* $0.1 \leq t \leq 2.3$ *for a wavy crack subjected to a uniform stress* $\sigma_{\mathrm{II}}^{\infty}$ *at infinity.*

This example is also well conditioned. We choose $\gamma_1 = e^{0.8i}$ and $\gamma_2 = e^{0.9i}$ as initial guesses. The GMRES iterative solver typically converges to a residual of 10^{-14} in 17 iterations. After 11 iterations with Broyden's method, and with 272 discretization points, we find that $\gamma_1 = e^{it_1}$ and $\gamma_2 = e^{it_2}$, where $t_1 = 0.8084089984688$ and $t_2 = 0.8751062182394$, make the solution to (60, 61) satisfy (29) and (32–34); see Figure 3. With 272 discretization points this calculation took 40 seconds on a SUN Ultra 10 workstation.

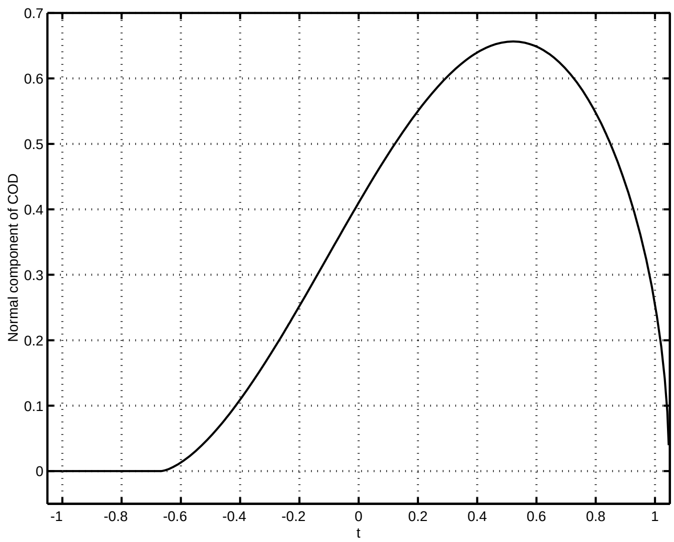

FIG. 4. *Example* 4*: The normal component of the crack-opening displacement versus arclength parameter* $-\pi/3 \leq t \leq \pi/3$ *for a unit circular arc–shaped crack subjected to a uniform stress* $(\sigma_{\rm I}^{\infty} + \sigma_{\rm II}^{\infty} + \sigma_{\rm III}^{\infty})/2$ *at infinity.*

TABLE 1

Convergence of the contact angle η *under uniform overresolution. The geometry is the circular arc–shaped crack in Example* 4*. The correct value, calculated in quadruple precision arithmetic, is* $\eta = 21.77476653838534$.

No. points	Contact angle η in degrees
48	21.77447948548968
64	21.77476653838650
96	21.77476653838545
160	21.77476653838534
320	21.77476653838536
640	21.77476653838539
1280	21.77476653838573
2560	21.77476653838509

Example 4: Circular arc–shaped crack with contact at crack tip. In this last example we change the parameterization of the crack to

$$z(t) = e^{it}\,, \qquad -\pi/3 \leq t \leq \pi/3\,. \tag{77}$$

A uniaxial stress $(\sigma_{\rm I}^{\infty} + \sigma_{\rm II}^{\infty} + \sigma_{\rm III}^{\infty})/2$ is applied at infinity. This corresponds to a clockwise rotation of the applied field in the three previous examples by $\pi/4$. As it turns out, the solution exhibits $\gamma_1 = \gamma_{\rm s}$. This example has previously been studied by Chao and Laws [1]. The GMRES iterative solver typically converges to a residual of 10^{-14} in 10 iterations. With $\gamma_2 = e^{-0.52i}$ as an initial guess, with seven iterations with the secant method, and with 64 discretization points, we find that $\gamma_2 = e^{it_2}$, where $t_2 = -0.6671561812487$, makes the solutions to (60), (61) satisfy (29) and (32)–(34). See Figure 4 for a plot of the normal component of the crack-opening displacement, and Table 1 and Figure 5 for a convergence study of the contact angle $\eta = \pi/3 + t_2$, expressed in degrees, under increased uniform resolution. With 64 discretization points the calculation took only one second on a SUN Ultra 10 workstation.

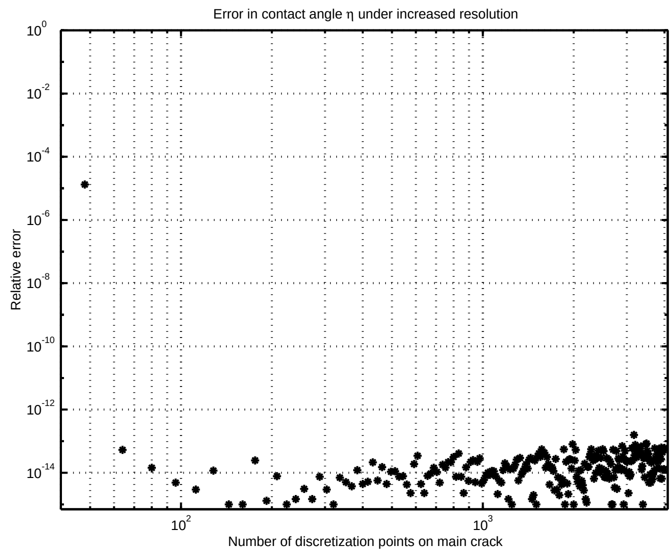

FIG. 5. *The relative error in the contact angle* η *under uniform overresolution. The geometry is the circular arc–shaped crack in Example* 4. *The reference value,* $\eta = 21.77476653838534$, *was calculated in quadruple precision arithmetic. A tolerance of* $5 \cdot 10^{-16}$ *for the residual was used as a stopping criterion in the GMRES iterative solver and for the function* f_2 *of* (66) *in the secant method iterations. Occasionally, larger tolerances had to be accepted in the secant method iterations in order to ensure convergence.*

Note how stable the convergence is in Table 1 and Figure 5. The problem is very well conditioned and the condition number of the system matrix reflects this (since we use a Fredholm second kind integral equation formulation). In fact, the condition number of the system matrix, defined as the ratio of the largest to the smallest singular value of the system matrix, is around 20. This means that the solution, in theory, can be computed with a relative error not worse than $20 \cdot \epsilon_{\mathrm{mach}}$. In IEEE double precision arithmetic this is approximately equal to $3 \cdot 10^{-15}$. Figure 5 indicates that our algorithm is close to this ideal.

Comparison with previous numerical results. It is interesting to compare our result in Example 4 with those of Chao and Laws [1]. These authors present graphical results for a quantity called "ratio of contact length" Δ. This quantity is defined in terms of a "polar angle subtended by contact zone" η and a "half-angle subtended by crack" ϕ as (Chao and Laws, private communication, 1998)

$$\Delta = \frac{\tan(\eta/2)}{\tan(\phi/2)}\,. \tag{78}$$

For the setup in our Example 4, Chao and Laws [1] report $\Delta \approx 0.40$, which corresponds to $\eta \approx 26$ degrees. No error estimate is given.

Torstenfelt [17] has developed a general purpose finite element program called "Trinitas" that is capable of solving frictionless contact problems in linear elasticity. As an independent test, we asked Daniel Hilding of the Department of Mechanical Engineering at Linköping University, Sweden, to perform as accurate a calculation as possible with Trinitas. The finite element method, used by Hilding to solve the frictionless contact problem, is a mixed variational method described in [8]. The method is shown to give approximations that converge to the solution, as the mesh is refined, for an elastic body in contact with a rigid obstacle. The necessary modifications of the finite element method needed in the present situation are found in [5]. In short, they can be described as follows.

A mixed variational inequality formulation of the contact problem was used in which both the displacement and the contact pressure are treated as unknowns. The displacement is approximated using isoparametric 9-node Lagrangian elements. The pressure is approximated using Simpson's rule. The resulting discrete variational inequality problem is solved using a Newton method, which yields a very accurate solution of the *discrete* problem. No special method was used to deal with the singularities. To simulate the infinite region, a square domain (with appropriate boundary conditions) was used and the crack was placed in the middle. The side of the square region had a length of about eight times the length of the crack length. The mesh was of the "mapped" type, with increasingly smaller elements near the crack. A series of problems with increasingly refined meshes was solved. The solutions to these problems were compared to give an idea of the error in the final reported result.

Using 15,000 degrees of freedom and 60 seconds of computing time, Hilding reports $21.67 < \eta < 22.28$ degrees. Our result in Example 4, arrived at with 64 discretization points and one second of computing time, corresponds to $\eta = 21.77476653839$ degrees. See Table 1.

REFERENCES

[1] R. Chao and N. Laws, *Closure of an arc crack in an isotropic homogeneous material due to uniaxial loading*, Quart. J. Mech. Appl. Math., 45 (1992), pp. 629–640.

[2] L. Greengard and J. Helsing, *On the numerical evaluation of elastostatic fields in locally isotropic two-dimensional composites*, J. Mech. Phys. Solids, 46 (1998), pp. 1441–1462.

[3] J. Helsing and G. Peters, *Integral equation methods and numerical solutions of crack and inclusion problems in planar elastostatics*, SIAM J. Appl. Math., 59 (1999), pp. 965–982.

[4] N. J. Higham, *Accuracy and Stability of Numerical Algorithms*, SIAM, Philadelphia, 1996.

[5] D. Hilding, A. Klarbring, and J. Petersson, *Optimization of structures in unilateral contact*, Appl. Mech. Rev., 52 (1999), pp. 139–160.

[6] H. Hochstadt, *Integral Equations*, John Wiley & Sons, New York, 1973.

[7] W. Kahan, *Further remarks on reducing truncation errors*, Comm. ACM, 8 (1965), p. 40.

[8] N. Kikuchi and J. T. Oden, *Contact Problems in Elasticity: A Study of Variational Inequalities and Finite Element Methods*, SIAM, Philadelphia, 1988.

[9] L. M. Milne-Thompson, *Plane Elastic Systems*, Springer, Berlin, 1968.

[10] B. Muckenhoupt, *Some weighted weak-type inequalities for the Hardy-Littlewood maximal function and the Hilbert transform*, Indiana University Math. J., 26 (1977), pp. 801–816.

[11] N. I. Muskhelishvili, *Some Basic Problems of the Mathematical Theory of Elasticity*, P. Noordhoff Ltd., Groningen, The Netherlands, 1953.

[12] F. París, J. C. Caño, and J. Varna, *The fiber-matrix interface crack – a numerical analysis using boundary elements*, Internat. J. Fracture, 82 (1996), pp. 11–29.

[13] V. Rokhlin, *Rapid solution of integral equations of classical potential theory*, J. Comput. Phys., 60 (1985), pp. 187–207.

[14] Y. Saad and M. H. Schultz, *GMRES: A generalized minimal residual algorithm for solving nonsymmetric linear systems*, SIAM J. Sci. Stat. Comput., 7 (1986), pp. 856–869.

[15] D. I. Sherman, *On the problem of plane strain in non-homogeneous media*, in Non-homogeneity in Elasticity and Plasticity, W. Olszak, ed., Pergamon Press, London, 1959, pp. 3–20.

[16] P. S. Theocaris and N. I. Ioakimidis, *The inclusion problem in plane elasticity*, Quart. J. Mech. Appl. Math., 30 (1977), pp. 437–448.

[17] B. Torstenfelt, *An Integrated Graphical System for Finite Element Analysis, User's Manual Version* 2.0, Tech. Report LiTH-IKP-R-737, Linköping University, Linköping, Sweden, 1993.